basis of our measurements on Tm metal films. In Tm our valence-band spectra are essentially identical to XPS spectra,[6] showing weak $5d$ emission near the Fermi energy and $4f^{12}$ emission at higher binding energy. The partial-yield and CIS spectra with either $4f$ or $5d$ initial states are all similar to bulk $4d \rightarrow 4f$ absorption spectra.[8,9] Thus, the $4d^9 4f^{13}(5d6s)^3$ final state of the photon absorption can decay either to $4d^{10}4f^{11}(5d6s)^3$ + electron or to $4d^{10}4f^{12}(5d6s)^2$ + electron. These results also show that Tm has no unusual surface valence changes, a possibility raised by Wertheim and Crecelius.[2]

Finally, we note that a complete experimental demonstration of our assignment entails comparison with a known $4d^{10}4f^6 \rightarrow 4d^9 4f^7$ absorption spectrum. Such a spectrum is not obtainable from any bulk rare earth, and will require further measurements on Sm compounds in which Sm is known to be divalent. Ours is the first observation of this particular $4d \rightarrow 4f$ absorption spectrum.

In summary, we have presented the results of photoelectron spectroscopy measurements on Sm (and Tm) metal using photon energies in the range 50–250 eV, a range not previously used for any rare-earth metal. We find strong contributions to valence-band emission from $4d \rightarrow 4f$ absorption, followed by elastic Auger decay. By CIS spectroscopy we are able to isolate and observe the $4d \rightarrow 4f$ absorption spectra of both $4f^5$ and $4f^6$ surface Sm atoms, providing strong, direct spectroscopic evidence of surface valence mixing in evaporated Sm films. More generally, it appears that photoelectron spectroscopy using photon energies in the 50–250-eV range will be a powerful tool for studying the very interesting phenomenon of rare-earth surface-valence-change effects.

It is a pleasure to acknowledge R. M. Martin and T. Gustafsson for several helpful discussions. This work was partially supported by the National Science Foundation (under Contract No. DMR77 27489) in cooperation with the Basic Science Division of the Department of Energy.

[1]G. K. Wertheim and M. Campagna, Chem. Phys. Lett. 47, 182 (1977).
[2]G. K. Wertheim and G. Crecelius, Phys. Rev. Lett. 40, 813 (1978).
[3]G. J. Lapeyre, R. J. Smith, and I. Anderson, J. Vac. Sci. Technol. 14, 384 (1977).
[4]I. Lindau and W. E. Spicer, J. Electron Spectrosc. 3, 409 (1974).
[5]F. C. Brown, R. Z. Bachrach, and N. Lien, Nucl. Instrum. Methods 152, 72 (1978).
[6]Y. Baer and G. Busch, J. Electron Spectrosc. 5, 611 (1974).
[7]M. Campagna, E. Bucher, G. K. Wertheim, and L. D. Longinotti, Phys. Rev. Lett. 33, 165 (1974).
[8]T. M. Zimkina, V. A. Fomichev, S. A. Gribovskii, and I. I. Zhukova, Fiz. Tverd. Tela 9, 1447 (1967) [Sov. Phys. Solid State 9, 1128 (1967)]; V. A. Fomichev, T. M. Zimkina, S. A. Gribovskii, and I. I. Zhukova Fiz. Tverd. Tela 9, 1490 (1967) [Sov. Phys. Solid State 9, 1163 (1967)].
[9]R. Haensel, P. Rabe, and B. Sonntag, Solid State Commun. 8, 1845 (1970).
[10]A. F. Starace, Phys. Rev. B 5, 1773 (1972).
[11]Jack Sugar, Phys. Rev. B 5, 1785 (1972).
[12]J. L. Dehmer and A. F. Starace, Phys. Rev. B 5, 1792 (1972).
[13]A report focusing on this decay process in Ce will be made elsewhere (L. I. Johansson, J. W. Allen, T. Gustafsson, I. Lindau, and S. B. M. Hagström, to be published).

Transition from Type-II to Type-I Superconductivity with Magnetic Field Direction

H. W. Weber, J. F. Sporna, and E. Seidl
Atominstitut der Österreichischen Universitäten, A-1020 Vienna, Austria
(Received 11 August 1978)

We report on a new effect in superconductivity and demonstrate experimentally that, because of the correlation of the upper critical field H_{c2} with crystal directions in single-crystalline TaN samples (anisotropy effect), at certain fixed temperatures the material is a type-I superconductor near the [100] *and* a type-II superconductor near the [111] directions.

Previous experimental work on the magnetic properties of superconductors has shown that high-purity type-I superconductors ($\kappa < 1/\sqrt{2}$, $\rho_n \propto 1/l \rightarrow 0$) may be converted into type-II superconductors ($\kappa > 1/\sqrt{2}$), e.g., by alloying thallium to lead[1-3] or by introducing nitrogen into tantalum.[4]

This conversion is caused by the reduction of the electron mean free path l and the corresponding increase of the Ginzburg-Landau (GL) parameter κ as described by the Gor'kov-Goodman relation[5]:

$$\kappa = \kappa_0 + 2.37 \times 10^6 \rho_n \sqrt{\gamma}. \quad (1)$$

[κ_0 is the GL parameter of the pure material, $l \to \infty$; ρ_n is the normal-state resistivity (Ω m); and γ is the Sommerfeld constant (J m^{-3} K^{-2}).] Because of the temperature dependence of the generalized GL parameter $\kappa_1(T) \geq \kappa_1(T_c) = \kappa$, superconductors with $\kappa < 1/\sqrt{2}$ change their magnetic behavior at some temperature $T^* < T_c$ and show type-II superconductivity with a first-order transition at H_{c1} (often referred to as type-II/1 be-. havior[2,4] at low temperatures ($T < T^*$) and type-I superconductivity above this transition temperature ($T^* < T < T_c$).

Based on previous work[6] on the H_{c2} anisotropy in cubic superconductors (cf. also Ref. 7) and the recent observation of a marked anisotropy effect in a *Ta*N single crystal,[8] the prime interest of the present systematic investigation of the tantalum-nitrogen system was to study the impact of the anisotropy effect on the transition from type-I to type-II superconductivity at T^*. For this purpose a cylindrical [1$\bar{1}$0]-oriented tantalum crystal (Ta-0) was successively loaded with interstitially dissolved nitrogen. The data were taken using axial magnetization (H_c), residual resistivity (ρ_n), and ac susceptibility measurements in transverse magnetic fields as a function of crystal direction [$H_{c2}(\theta)$ below T^* and $H_c(\theta)$ above T^*]. As an example of these experiments and their evaluation needed to determine the material parameters of our system, the temperature dependence of the "isotropic," i.e., appropriately averaged [cf. below, Eqs. (3) and (4)], GL parameter $\bar{\kappa}_1$,

$$\bar{\kappa}_1(T) = \bar{H}_{c2}(T)/H_c(T)\sqrt{2}, \quad (2)$$

and a comparison with the Gor'kov-Goodman relation (1) are shown in Fig. 1. Samples Ta-4, -5, and -6 (not shown in the figure), which are type-II superconductors in the entire temperature range, enable a straightforward evaluation of $\bar{\kappa}_1(T)$ and, therefore, $\bar{\kappa}_1(T_c) = \kappa$. From these three data points the solid line shown on the right-hand side of Fig. 1 and representing the dependence of κ on ρ_n, which was measured independently, is obtained and used to determine κ for those samples (Ta-0–3) which are type-I superconductors near T_c. A comparison of this procedure with Eq. (1) yields $\kappa_0 = 0.33$ and $\gamma = 680$

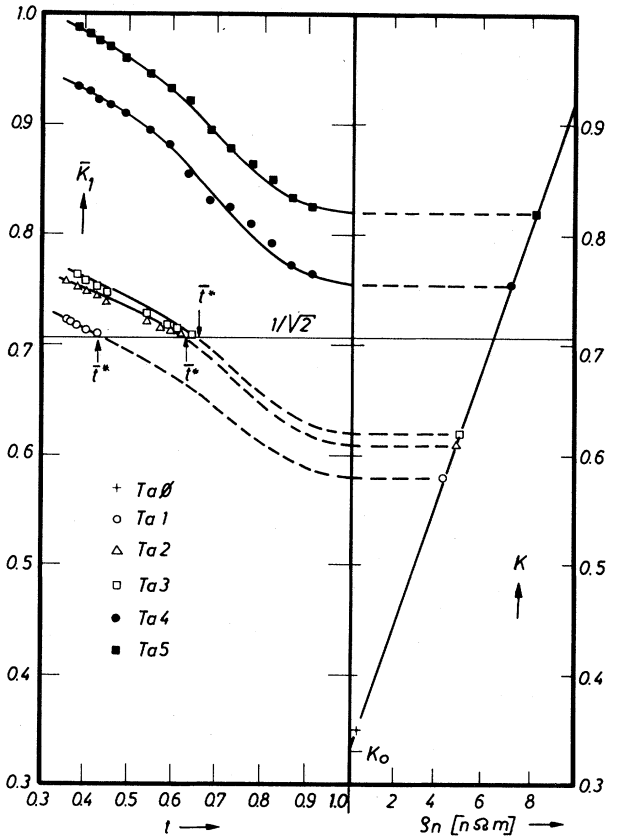

FIG. 1. Temperature dependence of the generalized GL parameter κ_1 and comparison of the κ-ρ_n dependence with Eq. (1) (solid line).

J m^{-3} K^{-2} in excellent agreement with previous data.[4,9] Detailed experiments on the angular dependence of the transition field into the normal conducting state were made on samples Ta-1–3 near the temperatures T^*. The results on Ta-1 are summarized in Figs. 2 and 3. At the lowest temperature shown in Fig. 2, $T = 1.65$ K, an undisturbed H_{c2} anisotropy pattern as usual for cubic superconductors (e.g., see Refs. 6 and 8) is observed. At $T = 1.70$ K, however, the isotropic thermodynamic critical field H_c just equals the upper critical field H_{c2} in the [100] direction. Therefore, in this direction the two phases, type-I and type-II superconductivity, are in equilibrium, κ_1 being just equal to $1\sqrt{2}$. With increasing temperature the angular range $\pm\Delta\theta$ from the [100] direction, where the sample is a type-I superconductor, increases, but the remaining directions around the [111] crystal orientation show still type-II superconductivity. At $T = 2.10$ K the [110] direction has become type-I superconducting as well, leaving only an angular range of $\pm 18°$

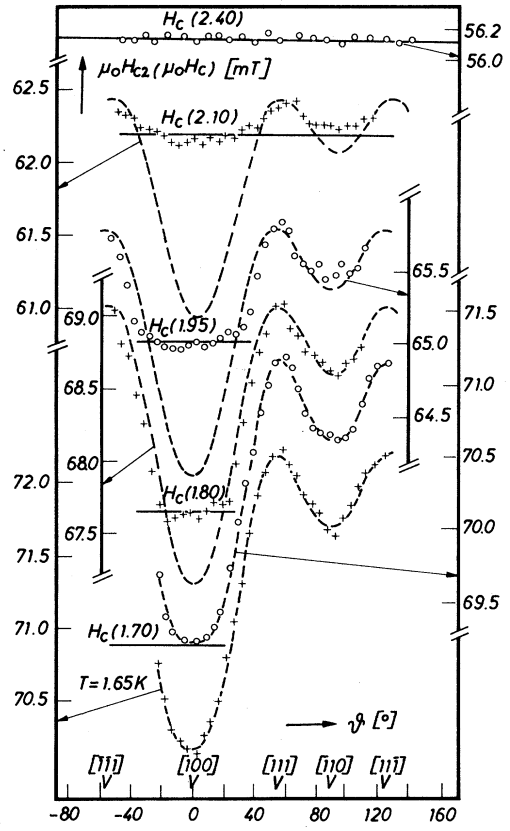

FIG. 2. Angular dependence of the transition field into the normal conducting state for Ta-1. The straight solid lines represent the thermodynamic critical fields $H_c(T)$; the broken lines represent computer fits using Eq. (3).

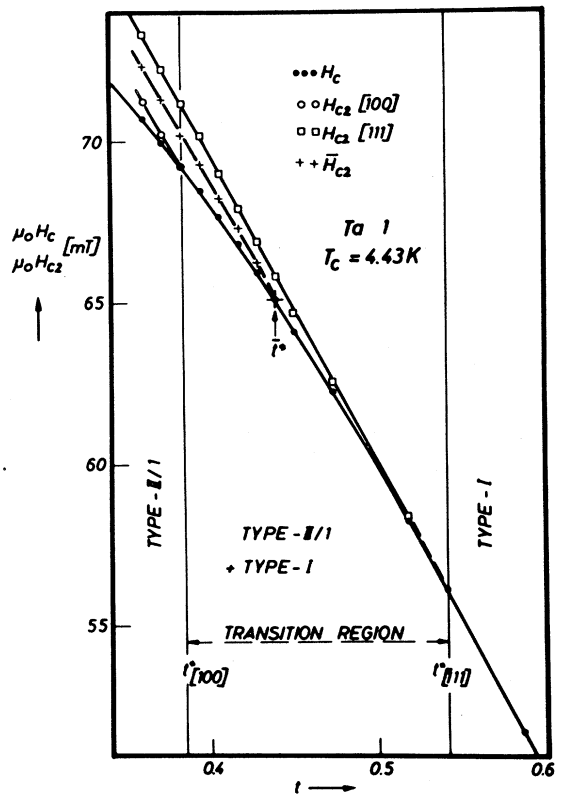

FIG. 3. Temperature dependence of the critical fields in the transition region.

around the [111] direction in the type-II superconducting state. Finally, at $T = 2.40$ K the transition to type-I superconductivity is completed at all crystal directions.

A plot emphasizing this transition region, where *whether the sample is a type-I or a type-II superconductor depends on which crystal direction is oriented parallel to the external field,* is shown in Fig. 3. The total transition width ΔT^* for Ta-1 is found to be remarkably large, $\Delta T^* = 0.70$ K. Furthermore, the dependence of $\bar{H}_{c2}$ and an average transition temperature $\bar{T}^*$ are shown in the figure, which were obtained in the following way. In the undisturbed type-II superconducting phase ($T < T_{100}{}^*$) the angular dependence of H_{c2} is analyzed in terms of cubic harmonic functions H_l (e.g., see Ref. 6),

$$H_{c2}(t, \alpha; \vec{e}_H) = \sum_{l=0,4,6,8} A_l(t, \alpha) H_l(\vec{e}_H) \qquad (3)$$

(t is the reduced temperature, α is the impurity parameter, $\vec{e}_H$ is the unit vector in the direction of the external field, and A_l are the anisotropy coefficients) with

$$A_0(t, \alpha) = \bar{H}_{c2}(t, \alpha). \qquad (4)$$

For $\vec{H} \perp [1\bar{1}0]$, which is always fulfilled in our geometry, the functions H_l may be expressed in terms of an angle θ through the relation $\vec{e}_{001} \cdot \vec{e}_H = \cos\theta$. Our analysis[8,10] shows first, that the coefficients A_6 and A_8 are negligibly small in the entire tantalum-nitrogen system, and secondly, that $-a_4 = A_4/A_0$ decreases linearly with temperature *towards* T_c and, therefore, remains finite upon approaching $T_{100}{}^*$, in agreement with Ref. 3. Furthermore, since $A_6, A_8 \approx 0$, and $H_4(\vec{e}_H) = 0$ for $\theta = 29.67° \sim 30°$, we obtain

$$H_{c2}(t, \alpha; \theta = 30°) = A_0(t, \alpha) = \bar{H}_{c2}(t, \alpha), \qquad (5)$$

As a result of the transition from type-I to type-II superconductivity at $t^*(\theta) = T^*(\theta)/T_c$,

$$H_{c2}(t^*(\theta), \alpha; \theta) \equiv H_c(t^*, \alpha), \qquad (6)$$

and combining Eqs. (5) and (6), we obtain

$$H_{c2}(\bar{t}^*, \alpha; \theta = 30) = \bar{H}_{c2}(\bar{t}^*, \alpha) = H_c(\bar{t}^*, \alpha). \qquad (7)$$

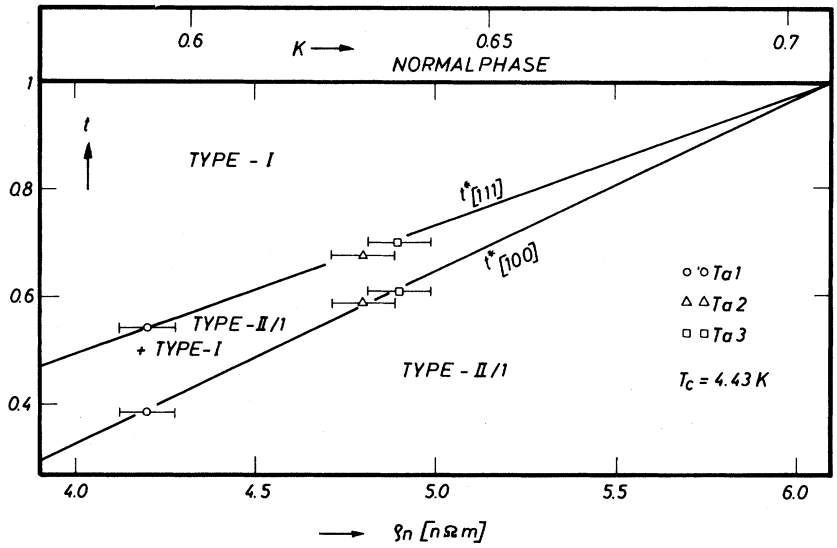

FIG. 4. Phase diagram showing the new phase boundaries between type-I and type-II/1 superconductivity in the tantalum-nitrogen system.

Hence,

$$\bar{t}^* = t^*(\theta = 30). \tag{8}$$

Equation (8) defines an appropriately averaged transition temperature $\bar{t}^*$, which is also shown in Figs. 1–3.

The dashed lines in Fig. 2 represent the angular dependence of H_{c2} according to Eq. (3), which would be observed in the *absence* of a transition to type-I superconductivity at $T^*(\theta)$. They were obtained in the following way. First, the low-temperature data ($T \leq 1.70$ K) were fitted by a least mean-square procedure to Eq. (3) with $A_{6,8} = 0$ to obtain $A_0(t)$ and $A_4(t)$. The result of these fits are shown for $T = 1.65$ and 1.70 K in Fig. 2. Then $a_4(t)$ was extrapolated linearly (cf. above) into the transition region; the extrapolation of $A_0(t)$ into this temperature range was achieved either through Eq. (7) or using the experimental results on $H_c(t)$ and the temperature dependence of $\kappa_1(T)$ shown in Fig. 1. The values of $A_{0,4}(t)$ obtained in this way were used to calculate $H_{c2}(t, \theta)$ in the entire angular range. It will be noted from Fig. 2 that this procedure describes the angular dependence of H_{c2} in the type-II superconducting crystal directions very well.

The corresponding experiments on samples Ta-2 and -3 qualitatively show the same behavior. As a result of the increased impurity content, T^* is shifted to higher temperatures (Fig. 1), the total width ΔT^* of the transition region becomes smaller, and the field modulation $H_{c2,111} - H_{c2,100}$ as well as the absolute values of the anisotropy coefficients $-a_4 = -A_4/A_0$ decrease correspondingly.

In summary, these experimental results demonstrate that a new variable has to be introduced into the low-κ side of the magnetic phase diagram in the tantalum-nitrogen system. As a result of the anisotropy effect, the phase boundary between type-II/1 and type-I superconductivity contains a region in the t-$\kappa(\rho_n)$ plane (Fig. 4), in which the type of superconductivity is characterized by having the crystal direction oriented parallel to the external field. Figure 4 shows that the total temperature intervals Δt^*, where this effect occurs, decrease with increasing GL parameter $\kappa(T_c)$ and disappear completely upon reaching $\kappa = 1/\sqrt{2}$. This experimental observation demonstrates the consistency of the data in a particularly clear way, since transitions to type-I superconductivity are obviously impossible for $\kappa > 1/\sqrt{2}$.

We wish to thank Professor H. Rauch for his continuous interest in the present work and Mr. H. Niedermaier for technical assistance.

[1]U. Krägeloh, Phys. Status Solidi 42, 559 (1970).
[2]U. Kumpf, Phys. Status Solidi (b) 44, 829 (1971).
[3]H. Kiessig, U. Essmann, H. Teichler, and W. Wiethaup, Phys. Lett. 51A, 333 (1975).
[4]J. Auer and H. Ullmaier, Phys. Rev. B 7, 136 (1973).
[5]B. B. Goodmann, IBM J. Res. Dev. 6, 63 (1962).
[6]E. Seidl, H. W. Weber, and H. Teichler, J. Low Temp. Phys. 30, 273 (1978).
[7]*Anisotropy Effects in Superconductors*, edited by

H. W. Weber (Plenum, New York, 1977).
[8]H. W. Weber, E. Seidl, and G. Kirschenhofer, Solid State Commun. 26, 795 (1978).
[9]J. I. Budnick, Phys. Rev. 119, 1578 (1960).
[10]J. F. Sporna, E. Seidl, and H. W. Weber, to be published.

Critical Dynamics and Spin Relaxation in a Cu-Mn Spin-Glass

M. B. Salamon
Department of Physics and Materials Research Laboratory, University of Illinois at Urbana–Champaign, Urbana, Illinois 61801
and
R. M. Herman
Division of Electrical Engineering, Brown University, Providence, Rhode Island 02912
(Received 21 July 1978)

A dramatic increase in the width of the exchange-narrowed paramagnetic resonance line in $Cu_{75}Mn_{25}$ is reported and shown to result from the critical dynamics of the spin-glass transition. The divergence of the linewidth as $(T_f - T)^{-1}$ is the first observation of power-law behavior at the spin-freezing temperature.

Spin-glass phases of magnetic alloys are generally recognized to result from the freezing of spin motion at a temperature T_f, without an accompanying appearance of long-range magnetic order.[1] While there is experimental evidence[2] for the slowing down of spin motion in spin-glasses, no singular behavior has yet been reported. In this Letter we present the results of electron paramagnetic resonance (EPR) measurements on a concentrated Cu-Mn alloy which show clearly, for the first time, power-law behavior of the critical dynamics associated with the spin-glass transition. Moreover, the behavior of this alloy is shown to be surprisingly close to that predicted by a time-dependent Ginzburg-Landau (TDGL) model proposed recently by Ma and Rudnick.[3]

As is well known, the linewidth of EPR signals in magnetic materials is dominated by exchange-narrowed dipolar broadening.[4] Korringa processes, dominant in dilute alloys, are estimated to contribute $\lesssim 10\%$ of the observed width, because of the strong "bottleneck" effect.[5] The relaxation rate T_2^{-1} is given approximately by

$$T_2^{-1} \sim \chi^{-1} \omega_d^2 \tau_s, \quad (1)$$

where χ is the static susceptibility; ω_d, the dipolar frequency $g^2\mu_B^2/\hbar v_s$; v_s, the volume per spin; and τ_s, the characteristic spin-spin relaxation time. Critical slowing down or speeding up[6] of τ_s increases or decreases χ/T_2, respectively. The critical behavior of χ tends to mask the effect of critical dynamics for ferromagnets, but the same is not true of antiferromagnets nor spin-glasses which have nonsingular susceptibilities. As we show below, the unique dynamics of the spin-glass transition, in which the relaxation time diverges while spatial correlations remain finite, leads to especially strong changes in the EPR linewidth.

Shown in Fig. 1 is the relaxation rate T_2^{-1} for a sphere of $Cu_{75}Mn_{25}$. The sample was quenched from high temperatures and subsequently maintained at 77 K except for experimental runs. The ac susceptibility[7] of an identical sample, also shown in Fig. 1, exhibits quite clearly the cusp associated with spin freezing at $T_f \simeq 115$ K. The initial dc susceptibility above T_f has Curie-Weiss-like behavior with a Weiss temperature $\Theta \simeq 97$ K.[8] EPR data, taken by conventional methods at 9.4

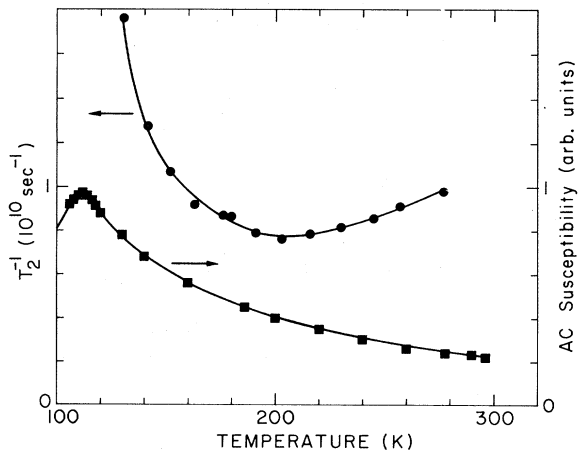

FIG. 1. Relaxation rate T_2^{-1} and ac susceptibility (Ref. 6) of quenched $Cu_{75}Mn_{25}$.